J. Chem. Thermodynamics 132 (2019) 164–173

Contents lists available at ScienceDirect

J. Chem. Thermodynamics

journal homepage: www.elsevier.com/locate/jct

Permittivity and electrical conductivity of copper oxide nanofluid (12 nm) in water at different temperatures

M.F. Coelho [a,b], M.A. Rivas [c], G. Vilão [a], E.M. Nogueira [a,b], T.P. Iglesias [c,*]

[a] Departamento de Física-Politécnico do Porto, Instituto Superior de Engenharia, Portugal
[b] CIETI-Centro de Inovação em Engenharia e Tecnologia Industrial, ISEP, Porto, Portugal
[c] Departamento de Física Aplicada, Facultad de Ciencias, Universidad de Vigo, Lagoas-Marcosende s/n, 36310 Vigo, Spain

ARTICLE INFO

Article history:
Received 31 July 2018
Received in revised form 10 December 2018
Accepted 12 December 2018
Available online 13 December 2018

Keywords:
Copper oxide
Electrical conductivity
Nanofluids
Nanoparticles
Relative permittivity
Ethylene glycol

ABSTRACT

The effective permittivity and electrical conductivity of copper oxide (12 nm) nanofluids in water are studied. The measurements were carried out at various concentrations (up to 2% in volume) and at six temperatures (from 298.15 K to 348.15 K). Empirical equations were used for describing the conductivity and the permittivity of the experimental data. The study shows the influence of the volume fraction, the temperature on relative permittivity and electrical conductivity. When compared with the previously published values for alumina (15 nm) in water, present results show the influence of the nanoparticle's nature. The enhancement of both permittivity and electrical conductivity were calculated and their behaviour was analysed. It is discussed whether their positive values can be considered greater than what would be expected. The contributions to permittivity from volume, contrast and interactions are separated. Theoretical models are applied in the study of permittivity and electrical conductivity. The poor predictions of classical models for permittivity are attributed to the positive behaviour of the permittivity change on mixing for these nanofluids. The contributions to electrical conductivity from water and nanoparticles are separated.

1. Introduction

Technological development has led scientists and engineers to make a constant research effort to achieve better results in the field of science and technology.

Since Choi in 1995, which demonstrated the increase in thermal conductivity in nanoparticle suspensions, several studies have shown that nanofluids have a higher thermal conductivity, higher electrical conductivity and light absorption. Thanks to all these properties, nanofluids have huge potential in industry: from refrigeration machines, motor cooling and electronic circuits [1,2] to solar heating of water and heating of buildings [3–6], as well as biomedical applications [7,8].

Much has been investigated regarding certain properties of nanofluids, such as thermal conductivity and, more recently, also viscosity in hybrid and non-hybrid nanofluids. With regard to the dielectric properties of water-based nanofluids, such as permittivity, some researchers have studied their behaviour with concentration and temperature. In [9,10], the permittivity behaviour of water-based nanofluids with γ-Al_2O_3 (15 nm) and (40 nm) with concentration up to 2% volume and temperatures from 298.15 K to 348.15 K was studied. Subramaniyan et al. [6] studied dielectric properties of TiO_2 with ethylene glycol, propylene glycol and water-based nanofluids at 293.15 K. They reported an increase in dielectric constant for all samples and the largest growth was observed for water-based nanofluids.

Some studies have been carried out on electrical conductivity in nanofluids. According to K. Sarojini [11], the electrical conductivity of a nanofluid is related to the ability of charged particles (ions) in the suspension to carry the charges (electrons) towards respective electrodes when an electric potential is applied. In nanofluids, the nanoparticles dispersed in a base fluid get charged due to the formation of electrical double layer (EDL) around the particle surface. These nanoparticles, together with the EDL, move towards an oppositely charged electrode when a potential is applied. This EDL formation depends on the surface charge, size and volume fraction of the particles and ionic concentration in the base fluid. Thus, the electrophoretic mobility of charged particles determines the electrical conductivity of a nanofluid. S. Ganguly et al. [12] studied the effective electrical conductivity of water-based α-Al_2O_3 nanofluids as a function of nanoparticle concentration and

* Corresponding author.
E-mail address: tpigles@uvigo.es (T.P. Iglesias).

https://doi.org/10.1016/j.jct.2018.12.025
0021-9614/

temperature. They found an almost linear increase in conductivity with increasing volumetric fraction as well as an increase in temperature for a given volumetric fraction. Maddah et al. [13] studied the electrical conductivity of silver and aluminum oxide nanofluids and reported significant increase when compared with the base fluid, which was water. Minea et al. [14] investigated electrical properties of aluminum oxide-water nanofluids too, and found a rise in electrical conductivity with an increase in volume fraction and temperature. Sikdar et al. [15] investigated TiO_2 nanofluids in water-based fluid and found an increase in electrical conductivity with an increase in volume concentrations, but they also observed a decrease in rate of increase with an increase in volume concentrations. Angayarkanni and Philip [16] showed an increase in electrical conductivity for α-Al_2O_3, SiO_2, γ-Al_2O_3, TiO_2 water-based nanofluids. They explain such a large increase as an effect of double electric layer surrounding each particle and particle size effect.

K. Sarogini et al. [11] detected an increase in electrical conductivity with increasing concentration and temperature ranging from 303 K to 333 K, for Cu (~80 nm), CuO (~80 nm), and Al_2O_3 (20–30 nm, 80 nm and 150 nm) in different base fluids (deionized water and ethylene glycol). Other authors have observed the same electrical conductivity behaviour in water-based nanofluids with different nanoparticles: Ganguly et al. [12] in water-based nanofluids with Al_2O_3 (13 nm); Minea et al. [14] in water-based nanofluids with Al_2O_3 (12 nm) between 298 K and 343 K; Sikdar et al. [15] in TiO_2 (21 nm) water-based nanofluids and T.T. Baby and Ramaprabhu [17] with water and ethylene glycol-based nanofluids of graphene with volume fractions between 0.005% and 0.056% at temperatures ranging from 298 K to 323 K.

Experimental studies of permittivity and electrical conductivity of nanofluids are of interest in understanding the dielectric properties of these colloids and to give operational values for some of the design parameters of machinery used in refrigeration and air-conditioning J. Koo [18]. The importance of electric properties of nanofluids as coolants is concisely explained in [19] and the references therein.

This paper presents the permittivity and electrical conductivity behaviour of a nanofluid consisting of 12 nm copper oxide particles in base water, in the temperature range (298–348) K and nanoparticle concentration up to 2%. No surfactant is added in the sample preparation to avoid masking the effect of nanoparticles and to allow these mixtures to be studied from the standpoint of view. The nanofluid under study was compared with the experimental values of γ-Al_2O_3 (15 nm) water-based nanofluid [9] obtained with the same experimental equipment and methods.

2. Materials and methods

2.1. Materials

Copper oxide nanoparticles (CuO) with an average particle size of 12 nm were supplied by Iolitec. The purity of these copper oxide nanoparticles stated by the supplier was greater than 0.995 mass fraction. The value of density stated by the supplier is 6.32 g·cm^{-3}. This value is in agreement with the value of 6.31 g·cm^{-3} from [20] for nanoparticles of (35–45) nm and that of 6.32 g·cm^{-3} from [21] for nanoparticles of (30–50) nm. The water was deionized and double distilled. Ethylene glycol was used without any further treatment. As it is hygroscopic after carried out the measures its water mass fraction was determined by Karl Fisher coulometer (Mettler Toledo DL 32). The provenance and purity of the materials studied are summarised in Table 1.

Table 1
Specifications for pure components.

Name	Copper Oxide (12 nm)	Water	Ethylene glycol
Chemical formula	CuO	H_2O	$C_2H_6O_2$
CAS number	1317-38-0	7732-18-5	107-21-1
Supplier	Iolitec	Deionized Double Distilled	Fluka
Mass fraction Purity	>0.995[a]		>0.995[a,b]

[a]Stated by the supplier.
[b]After carry out measures, without further treatment, the measured water content using a Karl Fisher coulometer (Mettler Toledo DL 32) was 927 × 10^{-6}.

2.2. Preparation of the nanofluids

In order to minimise errors in preparing the nanofluids, the nanoparticles were stored in airtight, opaque vials throughout the process to avoid contact with light and air.

The two-step method was used to prepare a copper oxide nanofluid sample in water at a certain volume fraction. The required amount of nanoparticle mass, which was calculated with the density provided by the manufacturer, was added to a certain amount of mass of base fluid. The copper oxide volume fraction, $\phi_{Cu,}$ was calculated by the equation (1), [9,10],

$$\varnothing_{CuO} = x_{CuO}V^*_{CuO}/\left[(1-x_{CuO})V^*_W + x_{CuO}V^*_{CuO}\right] \quad (1)$$

where x_{CuO} and V^*_{CuO} are the copper oxide mole fraction and molar volume, respectively. The molar volume of water was adjusted for experimental temperatures using standard density values [22].

All samples were prepared using a Mettler balance AE-240, which has a 0.00005 g accuracy and a resolution of ±0.0001 g. The quality of the base fluid was checked prior to each sample preparation at 298.15 K, using the commercial conductivity meter EC-Meter GLP 31 from CRISON. Then, in order to obtain uniform dispersion and prevent nanoparticle aggregation, a similar procedure to that used in [9,10] was followed. The Bandelin Sonoplus HD2200 (Bandelin Electronic, Berlin, Germany) ultrasonic homogeniser was used. Its 20 kHz oscillations are transmitted and amplified through a TT 13 titanium tip, 13 mm in diameter. This procedure was considered effective in [23] after comparing different sonication methods and was confirmed again in [24]. The sonication was applied during 60 min at 10% of maximum power. In order to prevent overheating, the sonication was applied in six time intervals of ten minutes, with a rest of three minutes between them, and the vial containing the sample was immersed in an ice bath throughout the sonication process. Although this method should prevent agglomeration during measurements, which were reproducible, the formation of small nanoparticle aggregates cannot be completely ruled out.

2.3. Apparatus and procedure

Complex relative permittivity at a given frequency is made up of two parts: $\varepsilon^*_r = \varepsilon_r - i\varepsilon_r''$. The real part ε_r represents the relative permittivity and the imaginary part ε_r'' is the so-called loss factor. The latter, which depends on the frequency, accounts for dielectric losses due to polarisation on the displacement current, ε_p'', and for the electrical conductivity due to actual charge transport according to:

$$\varepsilon_r'' = \frac{\sigma}{\varepsilon_o \omega} + \varepsilon_P'' \quad (2)$$

In this equation, σ is the conductivity of the nanofluid, ε_o = 8.8542 pF·m^{-1} is the permittivity of a vacuum and ω is the frequency of the applied electric field.

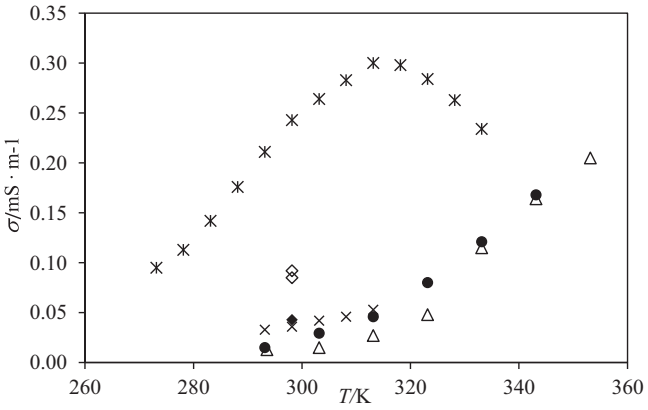

Fig. 1. Electrical conductivity, σ, of ethylene glycol as a function of temperature: *, [29]; ◇, [30]; ◆, [31]; x, [32]; ●, This work; Δ, [33].

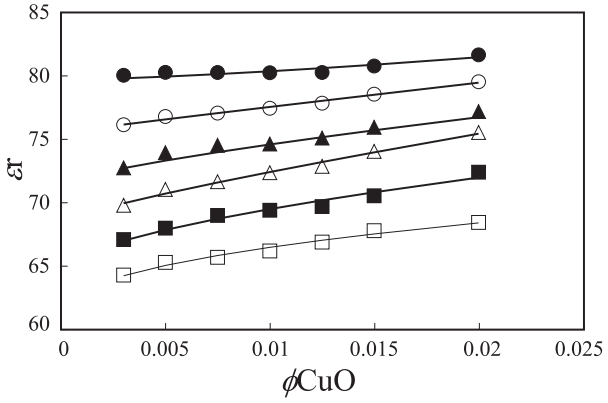

Fig. 2. Experimental relative permittivity, ε_r, of the CuO (12 nm) + water nanofluids as a function of copper oxide volume fraction, ϕ_{CuO}, at different temperatures: ●, T = 298.15 K; ○, T = 308.15 K; ▲, T = 318.15 K; △, T = 328.15 K; ■, T = 338.15 K; and □, T = 348.15 K. Continuous lines from the empirical equation (3).

The complex relative permittivity, ε_r^*, measurements were carried out at frequencies in the range of 1 kHz to 1 MHz using a HP4284A precision LCR Meter that was connected to a HP16452A measurement cell, which has parallel plate geometry, through a HP16452-61601 test lead. The equipment is fully automatic and computer-controlled by means of a HP-IB, [25]. The measurement cell was thermostated using a PolyScience fluid circulation bath, which controlled the temperature to within ±0.01 K.

The relative permittivity values, ε_r, were obtained at 1 MHz. The reliability of the measurements has been checked at this frequency [25–27], and an uncertainty less than 1% is estimated.

Measurements of electrical conductivity following the commercial specifications of the set up, mentioned above, are described in [28]. An equivalent procedure is followed in this work. The electrical conductivity is estimated from equation (2) by plotting ε_r'' against $1/\omega$. An average of 16 values for ε_r'' was obtained at each experimental frequency.

In order to check the quality of the experimental procedure, measurements were taken of standard solutions with conductivity 147 $\mu S \cdot cm^{-1}$, 1413 $\mu S \cdot cm^{-1}$ and 12.88 $mS \cdot cm^{-1}$ supplied by Crison and with 500 $\mu S \cdot cm^{-1}$ supplied by Fluka. The present method accurately reproduced all these values. Ethylene glycol supplied by Fluka with mass fraction purity > 0.995 and without any further treatment was also measured, Table S1 of the support material. Fig. 1 shows the values compared with those of the literature. The differences observed are probably due to the condition of the liquid. This procedure to measure the electrical conductivity has a combined expanded uncertainty of U_c = 1% at a 95% confidence level (k = 2), [9].

3. Results and discussion

3.1. Dielectric behaviour

Fig. 2 shows the effect of temperature and nanoparticle concentration on the relative permittivity of the {CuO (12 nm) + water} nanofluid. Relative permittivity decreases with increasing temperature and at fixed temperature increases slightly with increasing volume fraction. The numerical values are reported in Table S2 of the supporting material.

The relative permittivity data of the nanofluids in the experimental range of temperature and concentration is accurately described as a function of CuO volume fraction by the following empirical expression

$$\varepsilon_r = \varepsilon_{r,W} \exp\left[\beta (\phi_{CuO})^{\gamma}\right] \quad (3)$$

where $\varepsilon_{r,W}$ is the relative permittivity of the water, see Table S3 of the supporting material. The value of $\varepsilon_{r,W}$ at the two highest temperatures should be taken with caution because they differ up to 2% from those of literature. The best-fitting parameters, β and γ, are listed in Table 2 together with their corresponding standard deviations, s, calculated according to:

$$s = \left(\frac{\sum_i^N \left(y_{i,exp} - y_{i,calc}\right)^2}{N - k} \right)^{\frac{1}{2}} \quad (4)$$

where y and N are, respectively, the property values and the number of experimental data, k is the number of adjustable parameters used in the expression.

An alternative description as a function of both the CuO volume fraction and temperature can be performed by the following empirical equation, [34]

$$\mathrm{Ln}\varepsilon_r = \sum_i \sum_j \gamma_{ij} T^i \phi_{CuO}^j \quad (5)$$

the best-fitting parameters, γ_{ij}, and the standard deviation are listed in Table 3. We comment that these γ_{ij} values are only valid for CuO nanofluids within the experimental ranges of concentration and temperature. The behaviour at lower concentrations could be different as happen with thermal conductivity [35].

The behaviour of the nanofluid with temperature and concentration of the nanoparticles is similar to that obtained for alumina, Al_2O_3, of 15 nm and 40 nm in water nanofluids [9,10]. As the nature of the nanoparticles contributes to thermophysical properties of nanofluids, Fig. 3 compares the behaviour of {CuO (12 nm) + water} and that of {Al_2O_3 (15 nm) + water}, [9], because both nanofluids have the same base and nanoparticles of the similar size. Alumina (15 nm) in water nanofluids presented greater relative permittivity values at the experimental temperatures and, at

Table 2
Coefficients β and γ of equation (3) and their standard deviations, s, for CuO (12 nm) + water nanofluid at the different temperatures.

T/K	β	γ	s
298.15	4.852	1.376	0.27
308.15	1.992	0.936	0.15
318.15	1.231	0.726	0.44
328.15	2.109	0.786	0.19
338.15	0.972	0.558	0.29
348.15	0.564	0.399	0.19

Table 3
Coefficients γ_{ij} of equation (5) and the standard deviation, s, for CuO (12 nm) + water nanofluid.

γ_{00}	γ_{01}	γ_{02}	γ_{10}	γ_{11}	γ_{12}	s
5.6289	0.0710	0.0007	−0.0043	0.0180	−0.3375	0.01

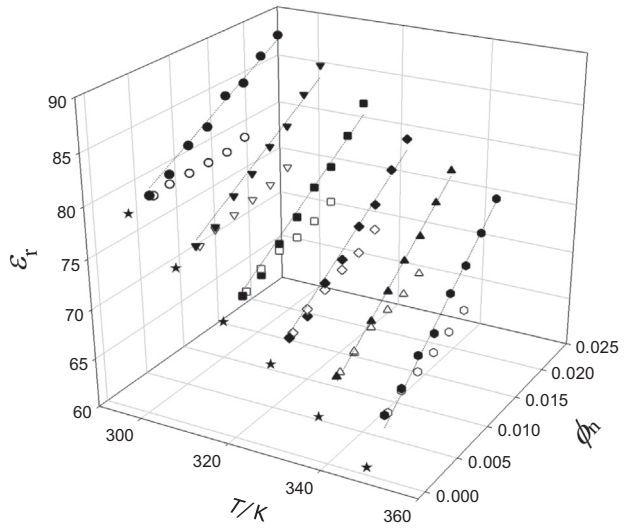

Fig. 3. Experimental relative permittivity, ε_r, of the CuO (12 nm) + water (open symbols) and γ-Al_2O_3 (15 nm) + water (filled symbols) nanofluids, [9], as a function of nanoparticle volume fraction, ϕ_n (n = CuO or Al_2O_3), and of temperature, T. Stars are for the relative permittivity of water. Curves, which were obtained from [9], are drawn as eye guides.

each temperature the nature of the nanoparticles has a greater influence at higher concentrations.

Fig. 4 shows the behaviour of permittivity enhancement, $\varepsilon_r/\varepsilon_{r,W}$, with the concentration of nanoparticles and temperature. The permittivity enhancement is slightly higher than that of the base fluid for all concentrations of copper oxide nanoparticles and increases with the nanoparticles concentration and temperature. The relative permittivity of solid CuO, $\varepsilon_{r,CuO}$, was considered insensitive

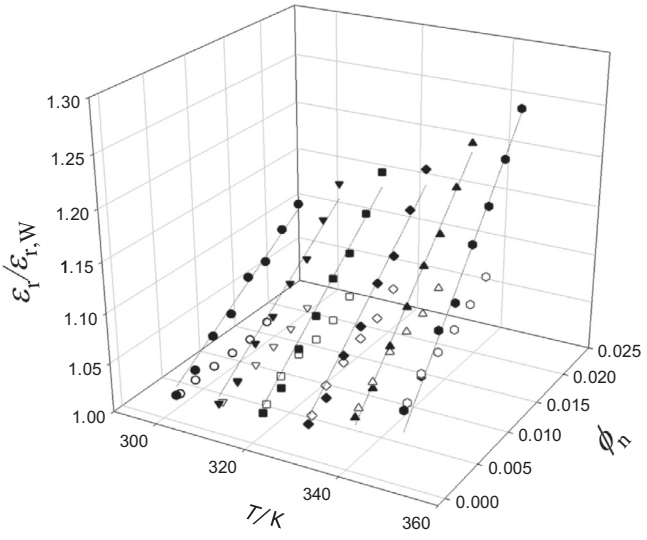

Fig. 4. Permittivity enhancement, $\varepsilon_r/\varepsilon_{r,W}$, for the CuO (12 nm) + water nanofluids (open symbols) and γ-Al_2O_3 (15 nm) + water nanofluids (filled symbols), [9], as a function of nanoparticle volume fraction, ϕ_n (n = CuO or γ-Al_2O_3), and of temperature, T. Curves, which were obtained from [9], are drawn as eye guides.

to temperature variation in the experimental range with a value of 18.1 at 2 MHz [22]. Note that as the relative permittivity of copper oxide is lower than that of the water, the permittivity of the nanofluid should be lower than the source fluid, which does not happen. The relative permittivity of alumina bulk (≈10) is also smaller than that of the water and the {γ-Al_2O_3 (15 nm) + water} nanofluid also shows values $\varepsilon_r/\varepsilon_{r,W} > 1$, [9].

Because the nature of the nanoparticles contributes to the permittivity enhancement, Fig. 4 compares the behaviour of this quantity with the change in temperature and concentration of nanoparticles, ϕ_n, for {CuO (12 nm) + water} and {γ-Al_2O_3 (15 nm) + water}, [9]. This Figure shows that the behaviours are similar for both systems but the values are smaller for the nanofluid with CuO nanoparticles. As the permittivity of copper oxide bulk is greater than that of alumina bulk the opposite would be expected.

To our knowledge, there are no studies in the literature related to the permittivity behaviour of (CuO + water) systems. There are some thermal conductivity studies that are of interest from the standpoint of view because of the parallelism in the mathematical formulation of magnitudes, permittivity and thermal conductivity. Therefore, we compared the permittivity enhancement to thermal conductivity enhancement. Thus, for water-based CuO (29 nm) nanofluids Mintsa et al. [36] show a thermal conductivity ratio of ∼1.04, at a 2% concentration and temperature of (294–296) K. Liu et al. [37] shows a ratio of ∼1.11 for CuO nanofluids (29 nm) based on ethylene at 2% concentration. Khedkar et al. [38] presents a ratio of ∼1.1 for water-based CuO (25 nm) nanofluids at 2% concentration and room temperature (299 K). It seems that at the volume concentration of 2% and room temperature the enhancement of thermal conductivity is the same order of magnitude as that of permittivity in the same experimental conditions.

The permittivity enhancement gives a direct estimate of the impact of the nanoparticles on the relative permittivity of the base fluid. However, according to a fundamental standpoint, the relative increment permittivity of mixing, $\Delta\varepsilon_r$, is more interesting. For fixed temperature and pressure, this property is defined by the equation (6), where $\phi_W = 1 - \phi_{CuO}$, ϕ_{CuO} is the volume fraction of copper oxide and $\varepsilon_{r,CuO}$ is the relative permittivity of bulk CuO.

$$\Delta\varepsilon_r = \varepsilon_r - (\phi_W\varepsilon_{r,W} + \phi_{CuO}\varepsilon_{r,CuO}) \quad (6)$$

For liquid mixtures, the sum within parenthesis is the ideal permittivity [39,40] and, in this case, equation (6) is the excess permittivity of the mixture.

In order to illustrate the application of equation (6) a temperature independent value of $\varepsilon_{r,CuO} = 18.1$ mentioned above was considered. The calculated values of $\Delta\varepsilon_r$ for copper oxide (12 nm) in water nanofluid are represented in Fig. 5. The $\Delta\varepsilon_r$ values are positive for all temperatures and concentrations, which means that the polarization is larger in the real mixture in relation to that of the ideal one. This behaviour is in line with the temperature dependence of the permittivity enhancement shown in Fig. 4. Fig. 5 shows that $\Delta\varepsilon_r$ increases with increasing temperature, which is an unusual behaviour when compared with that of the excess permittivity of the binary liquid mixtures. This last quantity, in general, tends to decrease with rising temperature [26,41,42]. In other words, the binary systems approach ideal behaviour when temperature increases. A positive behaviour of $\Delta\varepsilon_r$ that moves

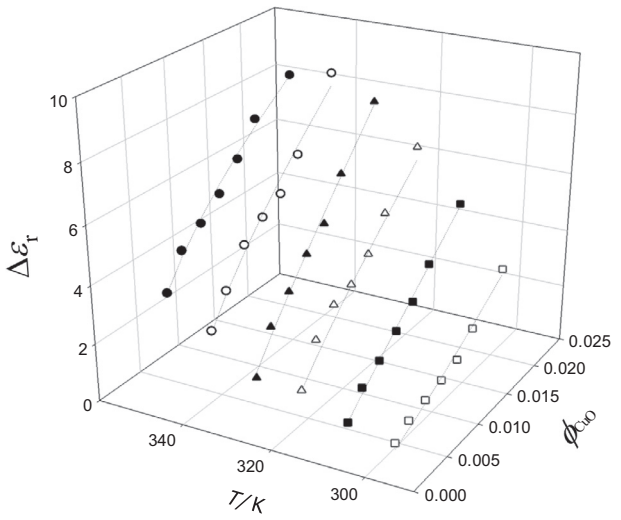

Fig. 5. Increment of permittivity of mixing, $\Delta\varepsilon_r$, for the CuO (12 nm) + water system as a function of copper oxide volume fraction, ϕ_{CuO}, at different temperatures: ●, T = 348.15 K; ○, T = 338.15 K; ▲, T = 328.15 K; △, T = 318.15 K; ■, T = 308.15 K; and □, T = 298.15 K. Continuous lines from equation (3).

away from ideal behaviour when rising temperature was also observed for the alumina water nanofluids studied in [9] and [10].

The model proposed in [43] was applied to $\Delta\varepsilon_r$ in order to study the contributions to this magnitude from the interactions, $\Delta\varepsilon_r^I$, from the dielectric contrast, $\Delta\varepsilon_r^C$ and from the excess volume, $\Delta\varepsilon_r^V$,

$$\Delta\varepsilon_r = \Delta\varepsilon_r^I + \Delta\varepsilon_r^C + \Delta\varepsilon_r^V \tag{7}$$

where

$$\Delta\varepsilon_r^C = -\varepsilon_{r,W}\frac{\phi_{CuO}(1-\phi_{CuO})(r_{CuO/W}-1)^2}{r_{CuO/W}+2+\phi_{CuO}(r_{CuO/W}-1)} \tag{7a}$$

and

$$\Delta\varepsilon_r^V = \frac{V_m^E}{V_m}[(\phi_W\varepsilon_{r,W}+\phi_{CuO}\varepsilon_{r,CuO})-1] \tag{7b}$$

$r_{CuO/W} = \varepsilon_{r,CuO}/\varepsilon_{r,W}$ is the contrast, V_m is the molar volume of the nanofluid and V_m^E is the excess molar volume calculated as

$$V_m^E = V_m - [x_{CuO}V_{CuO}^* + (1-x_{CuO})V_W^*] \tag{7c}$$

As $\Delta\varepsilon_r^C$, $\Delta\varepsilon_r^V$ and $\Delta\varepsilon_r$ are calculated from equation (7a), (7b) and (6) respectively, the values of $\Delta\varepsilon_r^I$ are determined from equation (7). The values of V_m^E/V_m were calculated from the extrapolation of density values for CuO (11 nm) + water [44] at the temperatures of this work. Concentrations of 1%, 1.75%, 2.5% and 5% by weight of CuO from [44] were considered in the extrapolation.

Fig. 6 shows the behaviour of $\Delta\varepsilon_r^I$ $\Delta\varepsilon_r^C$ and $\Delta\varepsilon_r^V$ for the CuO (12 nm) + water nanofluids at the extreme temperatures of 298.15 K and 348.15 K. $\Delta\varepsilon_r^I$ is temperature-dependent while $\Delta\varepsilon_r^C$ and $\Delta\varepsilon_r^V$ change slightly. $\Delta\varepsilon_r^I$ is responsible for the positive behaviour of $\Delta\varepsilon_r$ because $\Delta\varepsilon_r^C$ and $\Delta\varepsilon_r^V$ are small at these low working concentrations. In other words, interactions are essentially responsible for the permittivity behaviour. Fig. 6 shows as their influence increase with increasing temperature and concentration.

We have compared our experimental permittivity data with those predicted by certain theoretical models for binary dielectrics. Models of Looyenga, [45], Kraszewski [46], Iglesias-Peon [47] or Bruggeman [48] which, in general, acceptably predict permittivity of liquids mixtures, fail for these nanofluids. This information is reported in Table S4 of the supporting material. We have also tested the equation of Nan et al. [49] that was formulated for

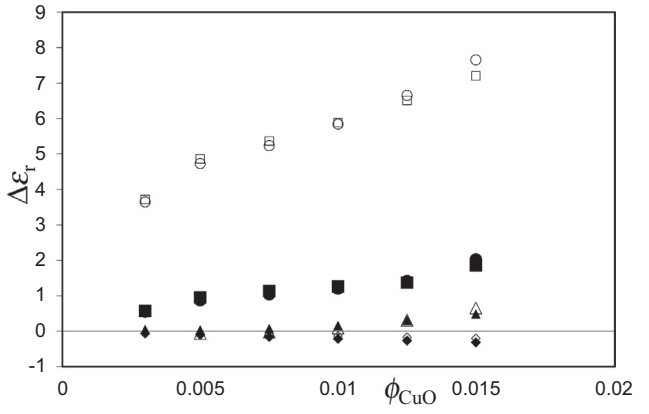

Fig. 6. $\Delta\varepsilon_r$, $\Delta\varepsilon_r^I$, $\Delta\varepsilon_r^C$ and $\Delta\varepsilon_r^V$ as a function of nanoparticle volume fraction, ϕ_{CuO} for the CuO (12 nm) + water system: $\Delta\varepsilon_r^I$ at temperatures T = 298.15 K, ■; T = 348.15 K, □; $\Delta\varepsilon_r^V$ at temperatures T = 298.15 K, ▲; T = 348.15 K, △; $\Delta\varepsilon_r$ at temperatures T = 298.15 K, ●; T = 348.15 K, ○; $\Delta\varepsilon_r^C$ at temperatures T = 298.15 K, ◆; T = 348.15 K, ◇.

predicting thermal conductivity of nanofluids containing carbon nanotubes and adapted for permittivity in [9,10]. This equation reads,

$$\varepsilon_r = \frac{3+\phi_{CuO}\left(\frac{\varepsilon_{r,CuO}}{\varepsilon_{r,W}}\right)}{3-2\phi_{CuO}}\varepsilon_{r,W} \tag{8}$$

As Table S5 shows, the equation prediction (8) is better than those from the classical models mentioned in Table S4, when the standard deviations are compared. Although the standard deviation with respect to theoretical values is the same for ε_r and $\Delta\varepsilon_r$, the latter allows a better visualization of the deviations of theoretical values with respect to the experimental ones. While the classical models predict a behaviour of $\Delta\varepsilon_r < 0$ at all concentrations, equation (8) predicts its positive behaviour correctly as in the case of {alumina (15 or 40 nm) + water} nanofluids, [9,10]. However, the experimental values of $\Delta\varepsilon_r$ increase when temperature is increased while the values predicted by this model decrease.

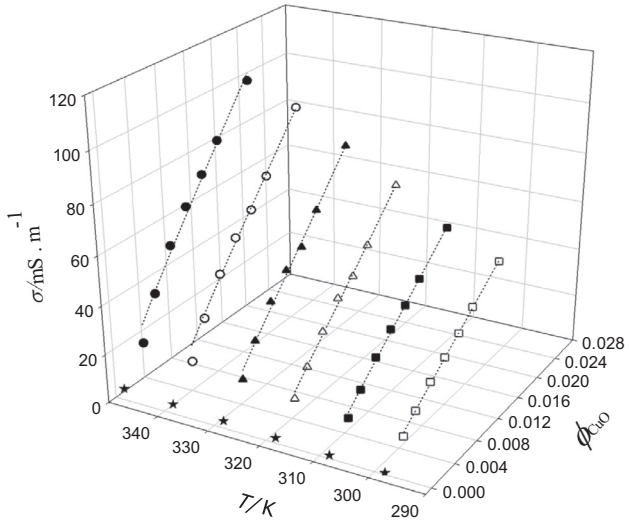

Fig. 7. Electrical conductivity, σ, of the CuO (12 nm) + water system as a function of CuO nanoparticle volume fraction, ϕ_{CuO}, and temperature, T: □, 298.15; ■, 308.15; △, 318.15; ▲, 328.15; ○, 338.15; ●, 348.15 K. Continuous lines calculated from equation (9). Stars are for the conductivity of water σ_W/mS·m^{-1} × 10.

3.2. Electrical conductivity behaviour

Fig. 7 shows the dependence of the experimental values of σ with ϕ_{CuO} and T. The conductivity increases with increasing copper oxide volume fraction at fixed temperature and with increasing temperature at fixed composition. The numerical values are reported in Table S6 of the supporting material. They can be accurately described in function of the nanoparticle concentration by the following empirical expression [9,10]

$$\sigma = \sigma_W \cdot \exp\left[\beta(\phi_{CuO})^{\gamma}\right] \quad (9)$$

where β and γ are fitting parameters and σ_W is the electrical conductivity of the water. Their values are given in Table 4 together with their corresponding standard deviations.

The electrical conductivity values for the CuO (12 nm) + water nanofluid are greater than those of γ-Al_2O_3 (15 nm) + water nanofluids [9]. This agrees with the results of K. Sarogini et al. [11] who studied electrical conductivity in CuO (80 nm) and α-Al_2O_3 (80 nm) nanofluids, both in deionized water.

Following the procedure used in [9] for describing the effect of concentration on electrical conductivity at fixed temperature by two-parameter empirical equations we have also taken the Archie's law, $\sigma = a \cdot \sigma_W(\phi_W)^m$ into consideration. However, this equation presents an average value of the standard deviations calculated at each temperature of 6 10^{-3} S·m^{-1}, which is large when comparing with those of Table 4. This empirical equation is inadequate in this case, perhaps because the conductivity of the base fluid, which is smaller than 1 mS·m^{-1} (see Table S6), is several orders of magnitude smaller than that of the nanoparticles, 0.064 S·m^{-1}, see [50]. The opposite occurred in the case of the {alumina (15 nm) + water} system, the electrical conductivity of the base fluid is about five orders of magnitude larger than that of the nanoparticles and this empirical equation predicts the experimental values properly, [9].

We have considered the Hill equation [51,52], which reads for electrical conductivity as

$$\sigma = \frac{K_0 \phi_{CuO}^n}{1 + K_0 \phi_{CuO}^n} \quad (10)$$

It has two fitting parameters, K_0 and n, and was used in different branches of science to quantitatively describe the degree of cooperation in different kinetic processes, [51–54], although some authors in the literature consider this equation as merely a fitting equation [55,56]. Table 5 shows these parameters and the standard deviation. Values of $n \neq 1$ would indicate that the CuO nanoparticles modify the electrical conductivity of the layer of water molecules that surround them. $n < 1$ would indicate that the first layer of molecules would tend to screen the effect of nanoparticles on the next water molecule layer. When $n > 1$ the opposite effect is produced and there would be positive cooperation. The molecules of the first layer would tend to enable the effect of CuO nanoparticles on the next molecular layer. This positive cooperation is also verified by the alumina (15 nm) + water system, [9], as shown in Table S7 of the supporting material.

Table 4
Coefficients β and γ of equation (9) and their standard deviations, s, for CuO (12 nm) + water nanofluid at the different temperatures, T.

T/K	β	γ	$s \cdot 10^3$/S·m^{-1}
298.15	11.289	0.147	0.8
308.15	11.029	0.156	1.3
318.15	11.023	0.169	1.8
328.15	10.725	0.170	2.4
338.15	10.094	0.158	1.4
348.15	9.939	0.158	4.3

The equation (11) that is named as equation of variable index [9] was also considered,

$$\sigma = \phi_W(\sigma_W)^i + \phi_{CuO}(\sigma_{CuO})^j \quad (11)$$

σ_{CuO} is the electrical conductivity of CuO bulk. This equation allows separating the contributions of the base fluid, $\phi_W(\sigma_W)^i$, from those of the nanoparticles, $\phi_{CuO}(\sigma_{CuO})^j$. According to [57], the electrical conductivity of CuO bulk at the temperature of 293 K is between (0.1–1) S·m^{-1}. In [50], a value of 0.064 S·m^{-1} is declared for pure CuO at room temperature and ranging from (0.18 to 0.39) S·m^{-1} for pressed powers in the range of temperatures of the present work. Because of the different values found in the literature for σ_{CuO}, the nominal value of 0.064 S·m^{-1} was considered in order to illustrate the application of equation (11). Table 5 shows the fitting parameters i, j at each temperature and the corresponding standard deviations. Fig. 8 shows these contributions. $\phi_W(\sigma_W)^i$ does not depend on concentration and slightly on temperature while $\phi_{CuO}(\sigma_{CuO})^j$ strongly depends on concentration but not on temperature. This last dependence is represented in Fig. 8 by a straight line. Only for the lowest nanoparticle concentration is the water contribution greater than that of the nanoparticles for some temperatures. A similar behaviour is found when the electrical conductivity values of pressed powers for CuO mentioned above are considered in equation (11). In this case, the predicted values from equation (11) also show standard deviations similar to those of Table 5.

Electrical conductivity enhancement defined as the ratio of the electrical nanofluid conductivity and the electrical conductivity of the base fluid (σ/σ_w), enables checking the change in behaviour of the electrical conductivity of the base fluid when different concentrations of nanoparticles are added. As can be seen in Fig. 9, the electrical conductivity enhancement increases with nanoparticle concentration at fixed temperature and decreases significantly with increasing temperature at fixed composition. The enhancement of electrical conductivities of alumina (15 nm) and copper oxide (12 nm) nanofluids in water are compared in Fig. 9 in terms of their nature.

The observed dependence on copper oxide content could be regarded as an expected behaviour because nanoparticles of greater conductivity than that of the base fluid are being added. In order to study whether the magnitude of the values $\sigma/\sigma_w > 1$ are an expect result or not, the mixing increment of electrical conductivity is considered, $\Delta\sigma$. This property is defined by equation (12) in a similar way as equation (6),

$$\Delta\sigma = \sigma - (\phi_W\sigma_W + \phi_{CuO}\sigma_{CuO}) \quad (12)$$

Fig. 10 shows the behaviour of $\Delta\sigma$ with the change in volume fraction concentration. The positive values of $\Delta\sigma$ at all volume fractions and temperatures would mean that the electrical conductivity is greater in the real mixture than that of the ideal one. That is to say, the positive behaviour of $\Delta\sigma$ indicates that the magnitude of the σ/σ_w values are greater than those that would be expected.

On the contrary, $\sigma/\sigma_w > 1$ in {alumina (15 nm) + water} nanofluid is an unexpected result because the electrical conductivity of the alumina does not exceed 5 pS·m^{-1}, which is about five orders of magnitude below that of the base fluid and $\Delta\sigma > 0$ for this system. The system with the highest electrical conductive enhancement is the one that has conductive nanoparticles.

In order to describe the variation with temperature an Arrhenius-type relationship has been considered in [59] which reads

$$\sigma = A \cdot \exp\left[-\frac{E_a}{RT}\right] \quad (13)$$

Table 5
Coefficients n and K_0 in Eq. (10), i and j in Eq. (11) and respective standard deviations, s, for CuO (12 nm) + water nanofluid at the different temperatures, T.

T/K	n	K_0	$s\cdot10^3$/(S·m^{-1})	i	j	$s\cdot10^3$/(S·m^{-1})
298.15	0.876	1.462	0.54	0.605	−0.278	0.88
308.15	0.880	1.799	0.83	0.627	−0.346	1.3
318.15	0.904	2.466	1.4	0.654	−0.423	1.7
328.15	0.885	2.726	2.1	0.636	−0.478	2.5
338.15	0.842	2.679	1.5	0.625	−0.531	3.2
348.15	0.823	2.808	2.9	0.588	−0.559	4.8

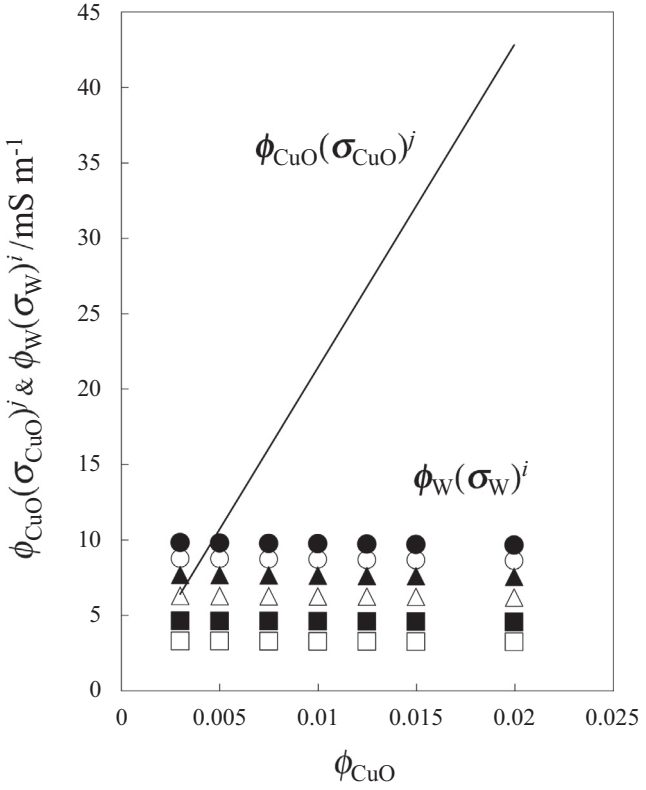

Fig. 8. Contributions to electrical conductivity, σ, from base fluid, $\phi_W(\sigma_W)^i$, and from nanoparticles, $\phi_{CuO}(\sigma_{CuO})^j$, for the CuO (12 nm) + water system as a function of CuO nanoparticle volume fraction, ϕ_{CuO}, and temperature, T. $\phi_{CuO}(\sigma_{CuO})^j$,continuous line. $\phi_{CuO}(\sigma_{CuO})^j$ symbols: □, 298.15; ■, 308.15; △, 318.15; ▲, 328.15; ○, 338.15; ●, 348.15 K.

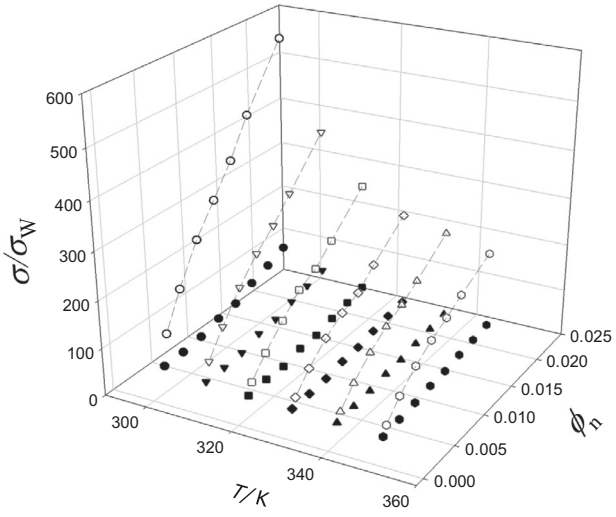

Fig. 9. Electrical conductivity enhancement, σ/σ_W, for the CuO (12 nm) + water (open symbols) and γ-Al_2O_3 (15 nm) + water (filled symbols) [9] nanofluids as a function of nanoparticle volume fraction, ϕ_n (n = CuO or γ-Al_2O_3), and temperature, T. Curves are drawn as eye guides.

where A is the pre-exponential or collision-frequency factor, E_a is the activation energy for electric conductivity and R is the gas constant.

In order to compare our results with those obtained in [9] we use an extension to the electrical conductivity of nanofluids of the classical Vogel–Fulcher–Tammann equation [60–62] originally developed for the temperature dependence of viscous flow, in the form

$$\sigma = A_{VFT} \cdot \exp\left[-\frac{B_{VFT}}{(T - T_g)}\right] \tag{14}$$

where T_g has the meaning of a glass transition temperature. The best values of this parameter are shown in Table 6. Given the similarity between equations (13) and (14), by equating the parameter B_{VFT} to E_a/R, we have estimated the activation energy values for conductivity shown in Table 6. As evidenced in Table 6, the analogue of the glass transition temperature increases with increasing CuO nanoparticle concentration. An opposite behaviour is observed for the activation energy. Furthermore, present activation energy values strongly suggest that the activation energy for the base fluids will be larger than for the corresponding nanofluids. Similar trends have been observed in [9] for {alumina (15 nm) + water} nanofluid

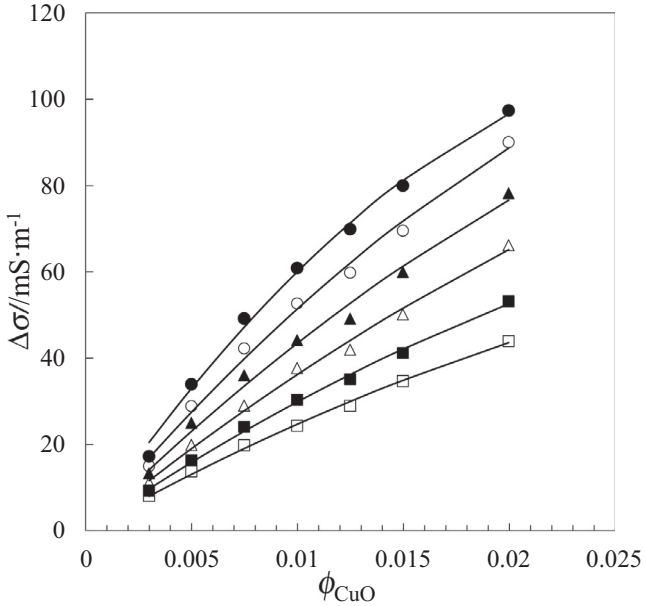

Fig. 10. Increment of electrical conductivity, $\Delta\sigma$, for the [CuO (12 nm) + water] nanofluids as a function of copper oxide volume fraction, ϕ_{CuO}, at different temperatures: □, 298.15; ■, 308.15; △, 318.15; ▲, 328.15; ○, 338.15; ●, 348.15 K. Solid lines by Redlich-Kister's [58] empirical equation are drawn as eye guides.

Table 6
Coefficients A_{VTF}, B_{VTF} and T_g in equation (14) and estimated energy, E_a, for the {CuO (12 nm) + water} system and the respective standard deviations, s, at the different volume fractions, ϕ_{CuO}.

ϕ_{CuO}	A_{VTF}/(S·m^{-1})	B_{VTF}/K	T_g/K	E_a/(J·mol^{-1})	$s\cdot10^3$/(S·m^{-1})
0.0030	0.203	498	143.7	4138	0.2
0.0050	0.454	482	161.2	4008	0.6
0.0075	0.604	457	165.1	3796	0.7
0.0100	0.665	428	168.4	3556	0.5
0.0125	0.677	399	172.5	3316	1.7
0.0150	0.625	347	178.6	2885	1.1
0.0200	0.616	294	185.5	2443	2.0

and in [63] for the activation energy of viscous flow of the {SiC (170 nm) + water} nanofluid. Comparing the results with those of [9] it is obtained that {T_g (CuO (12 nm) + water)} > {T_g (Al_2O_3 (15 nm) + water)} and {E_a (CuO (12 nm) + water)} > {E_a (Al_2O_3 (15 nm) + water)}.

4. Conclusions

From the experimental determination of relative permittivity and electrical conductivity of nanofluids of copper oxide particles (12 nm) in base water and with concentrations up to a volume fraction of 2% in the temperature range (298–348) K, we draw the following conclusions.

4.1. The effect of temperature and concentration

The relative permittivity decreases with increasing temperature and increases with increasing concentration. The permittivity enhancement ($\varepsilon_r/\varepsilon_{r,W}$) increases while increasing both temperature and concentration. The observed positive deviations of the relative permittivity in relation to its ideal value ($\Delta\varepsilon_r > 0$) indicate that the electrical polarization of real nanofluids is larger than the volume-fraction weighted average of pure component polarizations. The behaviour of this magnitude shows that the system tends towards the ideal behaviour when decreasing temperature and concentration. The positive behaviour of $\Delta\varepsilon_r$ may explain why equations such as Looyenga, Kraszewski, Iglesias-Peon or Bruggeman for prediction of permittivity failed to predict the permittivity of the present nanofluids. Indeed, these classical models lead to $\Delta\varepsilon_r < 0$. The Nan's model, explicitly formulated for nanofluids, obtains better results and predicts positive values of $\Delta\varepsilon_r$. However, this model fails to predict the behaviour of $\Delta\varepsilon_r$ with temperature. The reduction of $\Delta\varepsilon_r$ with the increase in temperature is predicted when the opposite occurs experimentally. The influence of both contrast and excess volume on the behaviour of $\Delta\varepsilon_r$ is smaller than the influence of the interactions that are essentially those responsible for the positive behaviour of this magnitude.

The electrical conductivity regularly increases when both copper oxide volume fraction and temperature increase. The variable index equation allows separating the contribution of CuO nanoparticles from that of the base fluid. The behaviour of nanofluid electrical conductivity comes from nanoparticles except at the lowest concentration. The change with temperature comes from base water. The Hill equation for electrical conductivity would indicate that the first layer of water molecules around the CuO nanoparticles would tend to enable the effect of CuO on the next water molecule layer.

The conductivity enhancement (σ/σ_W) increases with increasing CuO nanoparticle content at fixed temperature and decreases with increasing temperature at fixed composition. The observed positive deviations of the electrical conductivity in relation to its ideal value ($\Delta\sigma > 0$) indicate that the electrical conductivity of real nanofluids is greater than the electrical conductivity of the ideal mixture considering the latter as volume-fraction weighted average of pure component conductivities. The behaviour of this magnitude shows that the system tends towards the ideal behaviour when increasing temperature and decreasing concentration. Their positive values point out that the magnitude of the values of σ/σ_W are higher than those that would be expected.

4.2. The effect of the nanoparticle nature

The general trends described in Section 4.1 of ε_r and σ for {CuO (12 nm) + water} nanofluids follow the previously observed behaviours with temperature and concentration for {alumina (15 nm) + water}. Although the copper oxide permittivity is in the order of twice the alumina permittivity, the alumina nanofluids have higher permittivity values than those of copper oxide nanofluids. As the base fluid is the same in both systems, the pattern for permittivity is followed by $\varepsilon_r/\varepsilon_{r,W}$. The permittivity enhancement is greater than one which is unexpected because bulk permittivity of copper oxide, or alumina, is smaller than water permittivity. The influence of the nature of the nanoparticles on magnitudes, permittivity and permittivity enhancement is greater at higher concentrations.

The electrical conductivity of the (CuO + water) system is larger than that of the alumina + water, perhaps because the bulk conductivity of CuO is higher than that of the alumina. As the base fluid is the same in both systems, the pattern for conductivity is the same followed by σ/σ_W. The finding $\sigma/\sigma_W > 1$ is an expected result for the system with CuO nanoparticles because the σ of CuO is several orders of magnitude higher than that of the water. However, this is an unexpected result for the system with alumina nanoparticles because the σ of alumina is about five orders of magnitude below that of the water, [9]. The magnitude of σ/σ_W is greater for both systems than would be expected. Hill's model for electrical conductivity predicts positive cooperation of the first layer of water molecules for both systems, with CuO nanoparticles and with alumina nanoparticles.

Acknowledgements

We gratefully appreciate the financial support ED431C 2016-034 provided by the Xunta de Galicia (Spain). M.F.C. Thanks to the Instituto Superior de Engenharia do Porto for granting leave of absence to carry out experimental work at the Universidad de Vigo.

Appendix A. Supplementary data

Supplementary data to this article can be found online at https://doi.org/10.1016/j.jct.2018.12.025.

References

[1] A. Celen, A. Çebi, M. Aktas, O. Mahian, A.S. Dalkilic, S. Wongwises, A review of nanorefrigerants: flow characteristics and applications, Int. J. Refrig. 44 (2014) 125–140, https://doi.org/10.1016/J.IJREFRIG.2014.05.009.

[2] R. Saidur, K.Y. Leong, H.A. Mohammad, A review on applications and challenges of nanofluids, Renew. Sustain. Energy Rev. 15 (2011) 1646–1668, https://doi.org/10.1016/J.RSER.2010.11.035.

[3] W. Yu, D.M. France, S.U.S. Choi, J.L. Routbort, E. Systems, Review and assessment of nanofluid technology for transportation and other applications., Argonne, IL, 2007. doi: 10.2172/919327. 2.

[4] D. Wen, Y. Ding, Experimental investigation into convective heat transfer of nanofluids at the entrance region under laminar flow conditions, Int. J. Heat Mass Transf. 47 (2004) 5181–5188, https://doi.org/10.1016/J.IJHEATMASSTRANSFER.2004.07.01.

[5] S. Zeinali Heris, S.G. Etemad, M. Nasr, Esfahany, Experimental investigation of oxide nanofluids laminar flow convective heat transfer, Int. Commun. Heat Mass Transf. 33 (2006) 529–535, https://doi.org/10.1016/J.ICHEATMASSTRANSFER.2006.01.005.

[6] A. Subramaniyan, L.P. Sukumaran, R. Ilangovan, Investigation of the dielectric properties of TiO2 nanofluids, J. Taibah Univ. Sci. 10 (2016) 403–406, https://doi.org/10.1016/J.JTUSCI.2015.05.005.

[7] L. Zhang, F. Gu, J. Chan, A. Wang, R. Langer, O. Farokhzad, Nanoparticles in medicine: therapeutic applications and developments, Clin. Pharmacol. Ther. 83 (2008) 761–769, https://doi.org/10.1038/sj.clpt.6100400.

[8] R. Bawa, NanoBiotech 2008: exploring global advances in nanomedicine, Nanomedicine 5 (2009) 5–7 (accessed July 12, 2018) http://www.ncbi.nlm.nih.gov/pubmed/19230083.

[9] T.P. Iglesias, M.A. Rivas, R. Iglesias, J.C.R. Reis, F. Cohelho, Electric permittivity and conductivity of nanofluids consisting of 15 nm particles of alumina in base Milli-Q and Milli-Ro water at different temperatures, J. Chem. Thermodyn. 66 (2013) 123–130, https://doi.org/10.1016/J.JCT.2013.06.019.

[10] R. Iglesias, M.A. Rivas, J.C.R. Reis, T.P. Iglesias, Permittivity and electric conductivity of aqueous alumina (40 nm) nanofluids at different temperatures, J. Chem. Thermodyn. 89 (2015) 189–196, https://doi.org/10.1016/J.JCT.2015.05.021.

[11] K.G.K. Sarojini, S.V. Manoj, P.K. Singh, T. Pradeep, S.K. Das, Electrical conductivity of ceramic and metallic nanofluids, Colloids Surfaces A Physicochem. Eng. Asp. 417 (2013) 39–46, https://doi.org/10.1016/J.COLSURFA.2012.10.010.

[12] S. Ganguly, S. Sikdar, S. Basu, Experimental investigation of the effective electrical conductivity of aluminum oxide nanofluids, Powder Technol. 196 (2009) 326–330, https://doi.org/10.1016/J.POWTEC.2009.08.010.

[13] H. Maddah, M. Rezazadeh, M. Maghsoudi, S. NasiriKokhdan, The effect of silver and aluminum oxide nanoparticles on thermophysical properties of nanofluids, J. Nanostructure Chem. 3 (2013) 28, https://doi.org/10.1186/2193-8865-3-28.

[14] A.A. Minea, R.S. Luciu, Investigations on electrical conductivity of stabilized water based Al2O3 nanofluids, Microfluid. Nanofluidics 13 (2012) 977–985, https://doi.org/10.1007/s10404-012-1017-4.

[15] S. Sikdar, S. Basu, S. Ganguly, Investigation of electrical conductivity of titanium dioxide nanofluids, Int. J. Nanoparticles 4 (2011) 336–349, https://doi.org/10.1504/IJNP.2011.043496.

[16] S.A. Angayarkanni, J. Philip, Effect of nanoparticles aggregation on thermal and electrical conductivities of nanofluids, J. Nanofluids 3 (2014) 17–25, https://doi.org/10.1166/jon.2014.1083.

[17] T.T. Baby, S. Ramaprabhu, Investigation of thermal and electrical conductivity of graphene based nanofluids, J. Appl. Phys. 108 (2010), https://doi.org/10.1063/1.3516289 124308.

[18] J. Koo, C. Kleinstreuer, Laminar nanofluid flow in microheat-sinks, Int. J. Heat Mass Transf. 48 (2005) 2652–2661, https://doi.org/10.1016/J.IJHEATMASSTRANSFER.2005.01.029.

[19] M.Z. Bin Razali, M.S.A. Khiar, I.A. Zakaria, W.A.N.W. Mohamed, Effect of temperature towards electrical conductivities of low concentration of AL2O3 nanofluid in electrically active cooling system, in: 2014 IEEE Int. Conf. Control Syst. Comput. Eng. (ICCSCE 2014), IEEE, 2014, pp. 444–448. doi: 10.1109/ICCSCE.2014.7072760.

[20] A.H.A. Al-Waeli, M.T. Chaichan, H.A. Kazem, K. Sopian, Comparative study to use nano-(Al2O3, CuO, and SiC) with water to enhance photovoltaic thermal PV/T collectors, Energy Convers. Manage. 148 (2017) 963–973, https://doi.org/10.1016/J.ENCONMAN.2017.06.072.

[21] M. Zadkhast, D. Toghraie, A. Karimipour, Developing a new correlation to estimate the thermal conductivity of MWCNT-CuO/water hybrid nanofluid via an experimental investigation, J. Therm. Anal. Calorim. 129 (2017) 859–867, https://doi.org/10.1007/s10973-017-6213-8.

[22] D.R. Lide, Handbook of Chemistry and Physics, 90th ed., CRC Press, 2009.

[23] M.J. Pastoriza-Gallego, C. Casanova, R. Páramo, B. Barbés, J.L. Legido, M.M. Piñeiro, A study on stability and thermophysical properties (density and viscosity) of Al2O3 in water nanofluid, J. Appl. Phys. 106 (2009), https://doi.org/10.1063/1.3187732 064301.

[24] D. Cabaleiro, M.J. Pastoriza-Gallego, M.M. Piñeiro, L. Lugo, Characterization and measurements of thermal conductivity, density and rheological properties of zinc oxide nanoparticles dispersed in (ethane-1,2-diol + water) mixture, J. Chem. Thermodyn. 58 (2013) 405–415, https://doi.org/10.1016/J.JCT.2012.10.014.

[25] T.P. Iglesias, J.L. Legido, S.M. Pereira, B. de Cominges, M.I. Paz Andrade, Relative permittivities and refractive indices on mixing for (n-hexane + 1-pentanol, or 1-hexanol, or 1-heptanol) at T = 298.15 K, J. Chem. Thermodyn. 32 (2000) 923–930, https://doi.org/10.1006/JCHT.2000.0661.

[26] M. Rivas, S. Pereira, T. Iglesias, Relative permittivity of the mixtures (dimethyl or diethyl carbonate) + n-nonane from T=288.15 K to T=308.15 K, J. Chem. Thermodyn. 34 (2002) 1897–1907, https://doi.org/10.1016/S0021-9614(02)00260-4.

[27] S.M. Pereira, T.P. Iglesias, J.L. Legido, M.A. Rivas, J.N. Real, Relative permittivity increments for xCH3OH+ (1–x)CH3OCH2(CH2OCH2)3CH2OCH3 from T= 283.15 K to T= 323.15 K, J. Chem. Thermodyn. 33 (2001) 433–440, https://doi.org/10.1006/jcht.2000.0746.

[28] S. Choudhary, R.J. Sengwa, Ionic conduction in binary mixtures of dipolar liquids, J. Mol. Liq. 175 (2012) 33–37, https://doi.org/10.1016/J.MOLLIQ.2012.08.011.

[29] J. Fal, A. Barylyak, K. Besaha, Y.V. Bobitski, M. Cholewa, I. Zawlik, K. Szmuc, J. Cebulski, G. Żyła, Experimental investigation of electrical conductivity and permittivity of SC-TiO2-EG nanofluids, Nanoscale Res. Lett. 11 (2016) 375, https://doi.org/10.1186/s11671-016-1590-7.

[30] G. Żyła, J. Fal, Viscosity, thermal and electrical conductivity of silicon dioxide–ethylene glycol transparent nanofluids: an experimental studies, Thermochim. Acta 650 (2017) 106–113, https://doi.org/10.1016/J.TCA.2017.02.001.

[31] A. Yurquina, M.E. Manzur, P. Brito, R. Manzo, M.A.A. Molina, Solubility and dielectric properties of benzoic acid in a binary solvent: water-ethylene glycol, J. Mol. Liq. 108 (2003) 119–133, https://doi.org/10.1016/S0167-7322(03)00178-8.

[32] Y. Guo, T. Zhang, D. Zhang, Q. Wang, Experimental investigation of thermal and electrical conductivity of silicon oxide nanofluids in ethylene glycol/water mixture, Int. J. Heat Mass Transf. 117 (2018) 280–286, https://doi.org/10.1016/J.IJHEATMASSTRANSFER.2017.09.091.

[33] Z. Tan, H. Shen, S. Chen, Measurement of chemical and physical properties of 1,2-ethanediol and its aqueous solution, Chem. Eng. (China) (1983) 41–50.

[34] C.F. Riadigos, R. Iglesias, M.A. Rivas, T.P. Iglesias, Permittivity and density of the systems (monoglyme, diglyme, triglyme, or tetraglyme + n-heptane) at several temperatures, J. Chem. Thermodyn. 43 (2011) 275–283, https://doi.org/10.1016/J.JCT.2010.09.008.

[35] J. Eapen, R. Rusconi, R. Piazza, S. Yip, The classical nature of thermal conduction in nanofluids, J. Heat Transfer. 132 (2010), https://doi.org/10.1115/1.4001304 102402.

[36] H.A. Mintsa, G. Roy, C.T. Nguyen, D. Doucet, New temperature dependent thermal conductivity data for water-based nanofluids, Int. J. Therm. Sci. 48 (2009) 363–371, https://doi.org/10.1016/J.IJTHERMALSCI.2008.03.009.

[37] M.-S. Liu, M.C.-C. Lin, I.-T. Huang, C.-C. Wang, Enhancement of thermal conductivity with CuO for nanofluids, Chem. Eng. Technol. 29 (2006) 72–77, https://doi.org/10.1002/ceat.200500184.

[38] R.S. Khedkar, S.S. Sonawane, K.L. Wasewar, Influence of CuO nanoparticles in enhancing the thermal conductivity of water and monoethylene glycol based nanofluids, Int. Commun. Heat Mass Transf. 39 (2012) 665–669, https://doi.org/10.1016/J.ICHEATMASSTRANSFER.2012.03.012.

[39] T.P. Iglesias, J.C.R. Reis, L. Fariña-Busto, On the definition of the excess permittivity of a fluid mixture. II, J. Chem. Thermodyn. 40 (2008) 1475–1476, https://doi.org/10.1016/J.JCT.2008.04.011.

[40] J.C.R. Reis, T.P. Iglesias, G. Douhéret, M.I. Davis, The permittivity of thermodynamically ideal liquid mixtures and the excess relative permittivity of binary dielectrics, Phys. Chem. Chem. Phys. 11 (2009) 3977, https://doi.org/10.1039/b820613a.

[41] M.A. Rivas, T.P. Iglesias, S.M. Pereira, N. Banerji, On the permittivity and density measurements of binary systems of triglyme + (n-nonane or n-dodecane) at various temperatures, J. Chem. Thermodyn. 37 (2005) 61–71, https://doi.org/10.1016/J.JCT.2004.08.003.

[42] M.A. Rivas, A.H. Buep, T.P. Iglesias, Study of the binary mixtures of monoglyme + (hexane, cyclohexane, octane, dodecane) by ECM-average and PFP models, J. Chem. Thermodyn. 89 (2015) 69–78, https://doi.org/10.1016/J.JCT.2015.05.006.

[43] T.P. Iglesias, J.C.R. Reis, Separating the contributions of the volume change upon mixing, permittivity contrast and molecular interactions in the excess relative permittivity of liquid mixtures, Phys. Chem. Chem. Phys. 17 (2015) 13315–13322, https://doi.org/10.1039/C4CP05987E.

[44] M.J. Pastoriza-Gallego, C. Casanova, J.L. Legido, M.M. Piñeiro, CuO in water nanofluid: Influence of particle size and polydispersity on volumetric behaviour and viscosity, Fluid Phase Equilib. 300 (2011) 188–196, https://doi.org/10.1016/J.FLUID.2010.10.015.

[45] H. Looyenga, Dielectric constants of heterogeneous mixtures, Physica 31 (1965) 401–406, https://doi.org/10.1016/0031-8914(65)90045-5.

[46] A. Kraszewski, S. Kulinski, M. Matuszewski, Dielectric properties and a model of biphase water suspension at 9.4 GHz, J. Appl. Phys. 47 (1976) 1275–1277, https://doi.org/10.1063/1.322825.

[47] T.P. Iglesias, J. Peón Fernández, A new approach for prediction of the permittivity of mixtures, J. Chem. Thermodyn. 33 (2001) 1375–1381, https://doi.org/10.1006/JCHT.2001.0847.

[48] C. Böttcher, P. Bordewijk, Theory of Electric Polarization, Elsevier, Amsterdam, 1978.

[49] C.-W. Nan, Z. Shi, Y. Lin, A simple model for thermal conductivity of carbon nanotube-based composites, Chem. Phys. Lett. 375 (2003) 666–669, https://doi.org/10.1016/S0009-2614(03)00956-4.

[50] V.P. Zhuze, V. Kurchatov, The electrical conductivity of copper oxide, I n Phys. Z. Sowjetunion. 2 (1932) 453–467.
[51] A.V. Hill, The possible effects of the aggregation of the molecules of hemoglobin on its dissociation curves, J. Physiol. 40 (1910), iv–viii.
[52] S. Goutelle, M. Maurin, F. Rougier, X. Barbaut, L. Bourguignon, M. Ducher, P. Maire, The Hill equation: a review of its capabilities in pharmacological modelling, Fundam. Clin. Pharmacol. 22 (2008) 633–648, https://doi.org/10.1111/j.1472-8206.2008.00633.x.
[53] R. Gesztelyi, J. Zsuga, A. Kemeny-Beke, B. Varga, B. Juhasz, A. Tosaki, The Hill equation and the origin of quantitative pharmacology, Arch. Hist. Exact Sci. 66 (2012) 427–438, https://doi.org/10.1007/s00407-012-0098-5.
[54] D.L. Nelson, M.M. Cox, Lehninger Principles of Biochemistry, 6th ed., W.H. Freeman, New York, 2013.
[55] J.N. Weiss, The Hill equation revisited: uses and misuses, FASEB J. 11 (1997) 835–841, https://doi.org/10.1096/FASEBJ.11.11.9285481.
[56] J. Monod, J. Wyman, J.-P. Changeux, On the nature of allosteric transitions: a plausible model, J. Mol. Biol. 12 (1965) 88–118, https://doi.org/10.1016/S0022-2836(65)80285-6.
[57] G.V. Samsonov, The Oxide Handbook, New York-Washington-Lonfon, Ifi/Plenum, 1973.
[58] O. Redlich, A.T. Kister, Thermodynamics of nonelectrolyte solutions – x-y-t relations in a binary system, Ind. Eng. Chem. 40 (1948) 345–348, https://doi.org/10.1021/ie50458a035.
[59] L. Liu, Y. Yang, Y. Zhang, A study on the electrical conductivity of multi-walled carbon nanotube aqueous solution, Phys. E Low-Dimensional Syst. Nanostruct. 24 (2004) 343–348, https://doi.org/10.1016/J.PHYSE.2004.06.046.
[60] H. Vogel, The law of the relation between the viscosity of liquids and the temperature, Phys. Zeitschrift. 22 (1921) 645–646.
[61] G.S. Fulcher, Analisis of recent measurements of the viscosity of glasses, J. Am. Ceram. Soc. 8 (1925) 339–355, https://doi.org/10.1111/j.1151-2916.1925.tb16731.x.
[62] G. Tammann, W. Hesse, Die Abhängigkeit der Viscosität von der Temperatur bie unterkühlten Flüssigkeiten, Zeitschrift Für Anorg. Und Allg. Chem. 156 (1926) 245–257, https://doi.org/10.1002/zaac.19261560121.
[63] D. Singh, E. Timofeeva, W. Yu, J. Routbort, D. France, D. Smith, J.M. Lopez-Cepero, An investigation of silicon carbide-water nanofluid for heat transfer applications, J. Appl. Phys. 105 (2009), https://doi.org/10.1063/1.3082094 064306.

JCT 2018-637